

Visible light-driven photocatalytic benzoyl azides formation from benzotrichlorides using rhodium ion modified TiO₂

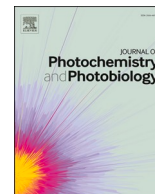
Shichijo, Keita

Shimakoshi, Hisashi

<https://hdl.handle.net/2324/7330151>

出版情報 : Journal of Photochemistry and Photobiology. 14, pp.100170-, 2023-04. Elsevier
バージョン :
権利関係 : Creative Commons Attribution-NonCommercial-NoDerivatives 4.0 International





Visible light-driven photocatalytic benzoyl azides formation from benzotrichlorides using rhodium ion modified TiO₂

Keita Shichijo, Hisashi Shimakoshi*

Department of Chemistry and Biochemistry, Graduate School of Engineering, Kyushu University, Fukuoka, 819-0395, Japan

ARTICLE INFO

Keywords:

Visible light
Metal ion modified TiO₂
Benzoyl azide
Photoredox reaction

ABSTRACT

Visible light-driven benzoyl azides formation catalyzed by a rhodium ion modified TiO₂ (Rh³⁺/TiO₂) is reported. The Rh³⁺/TiO₂ was prepared as a visible light responsive photocatalyst by a simple procedure from TiO₂ and RhCl₃·3H₂O. The Rh³⁺/TiO₂ exhibited a broaden visible light absorption from 400 nm to 600 nm. Benzoyl azide formation from a benzotrichloride and a trimethylsilyl azide (TMS-N₃) was performed catalyzed by the Rh³⁺/TiO₂ under visible light irradiation ($\lambda \geq 420$ nm) in air at room temperature. In this reaction, the benzotrichloride was effectively reduced by the single electron transfer (SET) from the Rh³⁺/TiO₂, and the benzoyl azide was produced in 71% yield via the reaction between the benzoyl chloride and TMS-N₃. In addition, several benzotrichloride derivatives were applied to this reaction and the corresponding benzoyl azide derivatives were formed in up to 71% yield. A kinetic analysis was also performed on these reactions, and it was suggested that the SET is the rate determining step in this reaction.

1. Introduction

Titanium oxide (TiO₂) is widely studied as an inexpensive and stable heterogeneous photocatalyst in the field of academia and the chemical industry [1–3]. In general, TiO₂ is excited by UV light irradiation to produce an excited electron (e⁻) on a conduction band (C.B.) and a hole (h⁺) on a valence band (V.B.) [4]. This electron–hole pair can promote a reductive reaction by electron (e⁻) and an oxidative reaction by hole (h⁺). Based on these properties of TiO₂, many examples of the UV light-induced photocatalytic reaction, such as environmental purification [5] and water splitting reaction [6], have been developed. However, the utilization of TiO₂ for organic synthesis is still rarely reported in spite of its significant importance [7,8]. Therefore, development of organic syntheses mediated by TiO₂ is strongly desired as green and sustainable molecular transformation processes.

In addition, the visible light-induced molecular transformation is interesting from the perspective for utilization of unlimited solar energy. However, the photocatalytic activity of TiO₂ requires UV light excitation, not visible light, because of a wide band gap ranging from 3.0–3.2 eV [4]. To overcome this problem, various kinds of TiO₂s have been developed as visible light responsive photocatalysts [9–11]. The modification of a metal ion on the TiO₂ surface is an effective method as a response to the visible light. Based on this, a metal ion modified TiO₂

(Mⁿ⁺/TiO₂) has been developed as a visible light responsive photocatalyst and applied to several photocatalytic reactions [12–14]. For instance, Kominami's group reported that the rhodium ion (Rh³⁺) modified TiO₂ (Rh³⁺/TiO₂) can effectively promote volatile organic compound (VOC) mineralization during visible light irradiation [15,16]. In addition, an earth abundant metal ion modified TiO₂ was prepared by Inoue's group to promote visible light-driven hydrogen evolution [17]. Based on these studies, the Mⁿ⁺/TiO₂ can be recognized as a photocatalyst for the visible light-driven organic synthesis.

Organic azides are valuable intermediates in the field of organic chemistry and biological chemistry [18]. In particular, acyl azides are important compounds due to their usefulness for organic synthesis and fundamental functional group transformations. The acyl azide can be rapidly converted to an isocyanate by the Curtius reaction and the isocyanate can react with amines, alcohols, and carboxylic acids to produce ureas, carbamates, and amides, respectively [19,20]. Therefore, the acyl azides play an important role in the formation of these N-containing compounds via new C–N bond construction. There are several types of general methodologies to prepare the acyl azide derivatives. The acyl azides are synthesized from acyl chlorides and a sodium azide (NaN₃) [21] or an organic azide source like as trimethylsilyl azide (TMS-N₃) [22] (Scheme 1 (a)). The acyl azides formation from carboxylic acids and a diphenyl phosphoric azide (DPPA) is also well known as a one-pot

* Corresponding author.

E-mail address: shimakoshi@mail.cstm.kyushu-u.ac.jp (H. Shimakoshi).

<https://doi.org/10.1016/j.jpap.2023.100170>

Available online 9 February 2023

2666-4690/© 2023 The Author(s). Published by Elsevier B.V. This is an open access article under the CC BY-NC-ND license (<http://creativecommons.org/licenses/by-nc-nd/4.0/>).

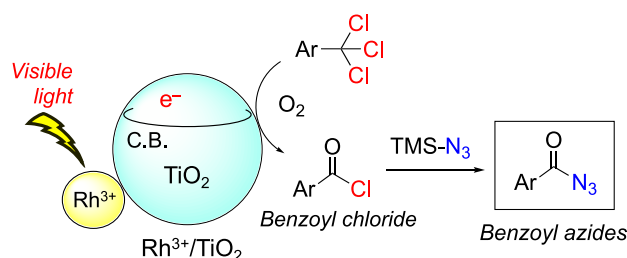


Fig. 1. Visible light-driven benzoyl azides formation mediated by the $\text{Rh}^{3+}/\text{TiO}_2$ under air.

synthetic methodology (Scheme 1 (b)) [23]. In this decade, the studies of novel synthetic methods for the acyl azide derivatives are progressing to develop a highly-efficient process. For example, the benzoyl azides formation from iodobenzenes with CO and NaN_3 readily occurs mediated by a Pd catalyst (Scheme 1 (c)) [24,25]. Yadav's group demonstrated the visible light-induced benzoyl azides formation from benzaldehydes as shown in Scheme 1 (d) [26]. It is the first example of the preparation of benzoyl azides directly from aldehydes employing visible light as an energy source. The visible light-driven methodologies for the acyl azides formation are still highly desirable as eco-friendly and sustainable preparations.

We have been developing a visible light-driven photo-reductive organic synthesis by using the metal ions modified TiO_2 [27,28]. Specifically, trichlorinated organic compounds were converted to amides in the presence of amines as a nucleophile by visible light irradiation in air. This methodology could possibly lead to further visible light-driven molecular transformations. In this paper, we propose visible light-driven benzoyl azides formation from benzotrichlorides catalyzed by the $\text{Rh}^{3+}/\text{TiO}_2$ as a novel visible light-driven photo-reductive organic synthesis (Scheme 1 (e)). In this reaction, the benzotrichlorides can be easily reduced by the single electron transfer (SET) from the $\text{Rh}^{3+}/\text{TiO}_2$ under visible light irradiation ($\lambda \geq 420$ nm), and the benzoyl azides can be produced with a one-pot reaction via the reaction between the benzoyl chlorides and TMS-N_3 (Fig. 1). This reaction can utilize oxygen (O_2) from air for construction of the acyl azide group and can proceed under mild conditions at ambient pressure and room temperature. Moreover, several benzotrichloride derivatives were also applied to this reaction and the corresponding benzoyl azides were formed in moderate yields. A mechanistic study including a kinetic analysis were also investigated in this paper.

2. Experimental

2.1. Measurements and equipment

The NMR spectra were recorded by a Bruker Avance 400 spectrometer at the Center of Advanced Instrumental Analysis of Kyushu University. The IR spectra were recorded by a Perkin-Elmer Spectrum Two using the ATR method. The UV-vis absorption spectra were measured by a Hitachi U-3300 spectrophotometer at room temperature. The diffuse reflectance (DR) UV-vis spectra were measured by a JASCO V-770 spectrophotometer equipped with a Φ 60 integrating sphere at room temperature. The X-ray fluorescence (XRF) analysis was done by a Shimadzu EDX-7000. The zeta potential was recorded by an Otsuka Electronics ELSZeno. The X-ray photoelectron spectroscopy (XPS) experiments were performed by a Shimadzu AXIS-ULTRA. The X-ray diffraction (XRD) was measured by the Rigaku SmartLab. The SEM image was acquired using a Hitachi SU8000 (acceleration voltage of 15 kV). TEM images were acquired using a JEOL JEM-2100F (acceleration voltage of 200 kV). The cyclic voltammograms (CV) were obtained using a BAS CV 50 W electrochemical analyzer. A three-electrode cell equipped with 1-mm diameter platinum wires as the working and counter electrodes was used. An Ag/AgCl (3.0 M NaCl aq.) electrode served as

the reference in the presence of tetrabutylammonium perchlorate ($n\text{-Bu}_4\text{NClO}_4$) as the supporting electrolyte. The HPLC spectra were obtained using a HITACHI ELITE LaChrom (Inertsil ODS-3 HPLC Column, 5 μm , 46×150 mm, solvent: H_2O and CH_3CN). A 200 W tungsten lamp with a 420 nm cut-off filter (Sigma Koki, 42 L) and a heat cut-off filter (Sigma Koki, 30H) were used as the light source for the visible light irradiation experiments. A black light, $\lambda_{\text{max}} = 365$ nm and 1.5 mWcm^{-2} , was used for the UV light irradiation.

2.2. Reagents and chemicals

All the solvents and chemicals used in this study were of reagent grade. Unless otherwise noted, commercial reagents were purchased from Tokyo Kasei Kogyo (TCI), Aldrich, Wako and other commercial sources. Titanium oxide (anatase, AMT-600, surface area = $52 \text{ m}^2\text{g}^{-1}$, diameter size = ca. 30 nm) was received from Tayca Co., Ltd. 3-Methylbenzotrichloride (7) was prepared according to the literature [29]. The products were isolated by chromatography (Silica Gel 60 N, spherical, neutral, Kanto Chemical) using hexane and ethyl acetate as the eluents, and identified by ^1H NMR, $^{13}\text{C}\{^1\text{H}\}$ NMR, and IR (ESI).

2.3. Synthesis and characterization of $\text{Rh}^{3+}/\text{TiO}_2$

The rhodium ion modified TiO_2 ($\text{Rh}^{3+}/\text{TiO}_2$) was synthesized based on the literature [28]. 1.0 g of anatase TiO_2 was refluxed in 10 mL of a rhodium chloride hydrate (0.16 mmol) aqueous solution for 2 h. After filtration of the solution, the obtained powder was washed three times with water to remove the chloride ion. The obtained powder was dried at 100°C for 24 h and calcinated at 200°C for 2 h to produce the $\text{Rh}^{3+}/\text{TiO}_2$.

The visible light absorption on the $\text{Rh}^{3+}/\text{TiO}_2$ was evaluated by Diffuse reflectance (DR)-UV-vis spectroscopy. The X-ray fluorescence (XRF) was measured to determine the loading amounts of the rhodium ion on the TiO_2 's surface. The zeta potential was also measured for the $\text{Rh}^{3+}/\text{TiO}_2$ in CH_3CN . The X-ray diffraction (XRD) and X-ray photoelectron spectroscopy (XPS) were carried out to investigate the surface and bulk properties of the $\text{Rh}^{3+}/\text{TiO}_2$, respectively. The microscopic morphologies of the $\text{Rh}^{3+}/\text{TiO}_2$ were investigated by SEM and TEM. The TEM-EDX mapping was also carried out for the $\text{Rh}^{3+}/\text{TiO}_2$.

2.4. General procedure of the benzoyl azide formation

The benzotrichloride (7.5×10^{-3} M), TMS-N_3 (7.5×10^{-2} M, 10 equiv.), *N,N*-diisopropylethylamine (*i*-Pr₂NEt) (5.0×10^{-2} M, 6.5 equiv.), and $\text{Rh}^{3+}/\text{TiO}_2$ (5.0 mg) were added to 10 mL of CH_3CN as a substrate, an azide source, a sacrificial reduction reagent, and a catalyst, respectively. The solution was stirred for 6 h during visible light irradiation ($\lambda \geq 420$ nm) in air at room temperature. The resulting solution was analyzed by HPLC to determine the product yields.

2.5. Kinetic study of the benzoyl azides formation

Several benzotrichloride derivatives were applied to the benzoyl azides formation under optimized conditions and the product yields were determined by HPLC every hour to establish a time profile. The rate equation for the consecutive reaction was used for the fitting on this time profile (Scheme 2)[30]. Concentration of the substrate was fitted by a single exponential function: $[\text{S}] = [\text{S}]_0 \exp(-k_1\tau)$, and generation of the product was fitted by a function: $[\text{P}] = [\text{S}]_0 \{k_1 / (k_2 - k_1)\} \{\exp(-k_1\tau) - \exp(-k_2\tau)\}$. k_1 and k_2 were defined as the producing rate constant (substrate $[\text{S}] \rightarrow$ product $[\text{P}]$; k_1) and as the over-reaction rate constant (product $[\text{P}] \rightarrow$ over-reacted product; k_2), respectively.

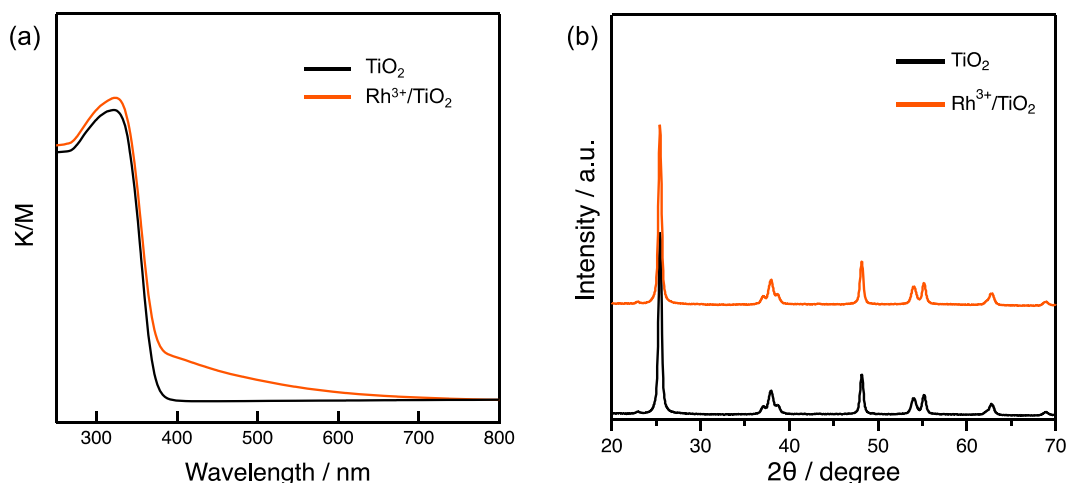


Fig. 2. (a) DR-UV-vis spectra of bare TiO_2 and $\text{Rh}^{3+}/\text{TiO}_2$, (b) XRD patterns of bare TiO_2 and $\text{Rh}^{3+}/\text{TiO}_2$.

Table 1

Diameter size, Rh^{3+} ion loading amount, and zeta potential of the catalyst.

Catalyst	Diameter size	Loading amount of Rh^{3+} ion	Zeta potential
$\text{Rh}^{3+}/\text{TiO}_2$	ca. 50 nm	$7.4 \times 10^{-5} \text{ mol g}^{-1}$	-78 mV

3. Results and discussion

3.1. Synthesis and characterization of $\text{Rh}^{3+}/\text{TiO}_2$

The rhodium ion modified TiO_2 ($\text{Rh}^{3+}/\text{TiO}_2$) was easily prepared based on Scheme 3. The $\text{Rh}^{3+}/\text{TiO}_2$ clearly exhibited a yellow color due to the modification of the rhodium ion on the surface of the TiO_2 (Fig. S1 (b)). To investigate the response to the visible light, the DR-UV-vis spectra were recorded for the bare TiO_2 and the $\text{Rh}^{3+}/\text{TiO}_2$. As shown in Fig. 2(a), a broad absorption was detected in the visible light region ($400 \text{ nm} \leq \lambda \leq 600 \text{ nm}$), which suggested that the $\text{Rh}^{3+}/\text{TiO}_2$ works as a visible light-responsive photocatalyst. According to the XRF analysis for the $\text{Rh}^{3+}/\text{TiO}_2$, it was found that 0.76 wt% ($7.4 \times 10^{-5} \text{ mol g}^{-1}$) of the rhodium ions were loaded on the TiO_2 's surface (Table 1). The zeta potential of the $\text{Rh}^{3+}/\text{TiO}_2$ was -78 mV in the CH_3CN (Table 1). The XRD patterns of the bare TiO_2 and the $\text{Rh}^{3+}/\text{TiO}_2$ are shown in Fig. 2(b).

The peaks, which are derived from the anatase type of TiO_2 [31], were maintained after the modification of the rhodium ions. The XPS spectrum for the $\text{Rh}^{3+}/\text{TiO}_2$ showed peaks from O 1s, Ti 2p_{1/2}, Ti 2p_{3/2}, Rh 3d_{3/2}, and Rh 3d_{5/2}. Especially, the Rh 3d_{3/2} and Rh 3d_{5/2} signals were detected at 314 eV and 309 eV, respectively [27,32]. It is suggested that the Rh^{3+} ions were fixed on the surface of the TiO_2 . Finally, the microscopic morphologies of the $\text{Rh}^{3+}/\text{TiO}_2$ were observed by the SEM and the TEM technologies. Many of the $\text{Rh}^{3+}/\text{TiO}_2$ nanoparticles were aggregated as shown in the SEM images (Fig. 3(a)). According to the TEM images, the single nanoparticles of the $\text{Rh}^{3+}/\text{TiO}_2$ were around 50 nm in diameter (Fig. 3(b)). Moreover, the TEM-EDX mapping was also carried out to reveal that the rhodium ions were uniformly modified on the TiO_2 's surface (Fig. 3(c)–(f)).

3.2. Photocatalytic benzoyl azide formation mediated by $\text{Rh}^{3+}/\text{TiO}_2$

The visible light-driven benzoyl azide formation was carried out in CH_3CN in the presence of the benzotrichloride (1) as a substrate, TMS-N_3 as the azide source, *N,N*-diisopropylethylamine (*i*-Pr₂NEt) as the sacrificial reduction reagent, and $\text{Rh}^{3+}/\text{TiO}_2$ as the catalyst. The results are summarized in Table 2. After several optimizations (Tables S1–S4), the benzoyl azide (2) was produced in 71% yield after 6 h of visible light irradiation (entry 1 in Table 2). As shown in entry 2, the yield of 2 was

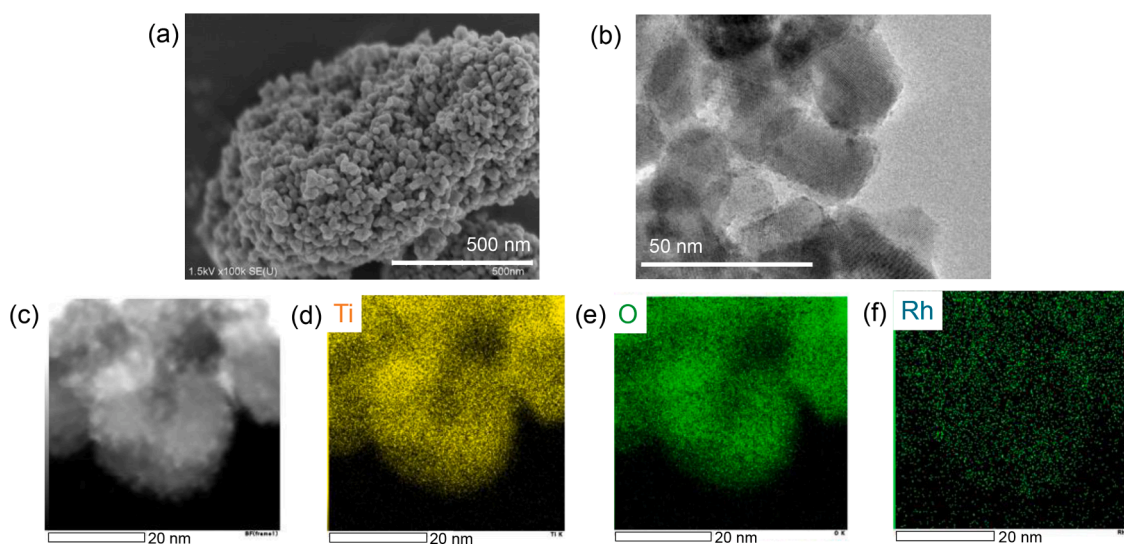


Fig. 3. (a) SEM image of $\text{Rh}^{3+}/\text{TiO}_2$, (b) TEM image of $\text{Rh}^{3+}/\text{TiO}_2$, (c) STEM image of $\text{Rh}^{3+}/\text{TiO}_2$, TEM-EDX mappings of $\text{Rh}^{3+}/\text{TiO}_2$; (d) Ti atom, (e) O atom, (f) Rh atom.

Table 2Benzoyl azide formation from benzotrichloride catalyzed by $\text{Rh}^{3+}/\text{TiO}_2$. [a]

Entry	Reaction conditions	Yield of 2 / %
1	as shown	71
2	without $\text{Rh}^{3+}/\text{TiO}_2$	2
3	without $i\text{-Pr}_2\text{NEt}$	0
4	without light	0
5 ^[b]	under N_2	7
6 ^[c]	under O_2	18
7 ^[d]	DPPA instead of TMS-N_3	48
8 ^[e]	NaN_3 instead of TMS-N_3	7
9 ^[f]	TiO_2 as catalyst	28
10 ^[g]	UV lamp instead of visible light	7
11 ^[h]	with 0.1 M DMPO	9
12 ^[i]	Recycled $\text{Rh}^{3+}/\text{TiO}_2$ as catalyst	61

[a] Conditions: $\text{Rh}^{3+}/\text{TiO}_2 = 5.0 \text{ mg}$ (Rh^{3+} ion: $2.7 \times 10^{-5} \text{ M}$), **1** = $7.5 \times 10^{-3} \text{ M}$, $[\text{TMS-N}_3] = 7.5 \times 10^{-2} \text{ M}$ (10 equiv.), $[i\text{-Pr}_2\text{NEt}] = 5.0 \times 10^{-2} \text{ M}$ (6.5 equiv.), solvent: CH_3CN , light source: 200 W tungsten lamp with 42 L cut-off filter ($\lambda \geq 420 \text{ nm}$) and a heat cut-off filter (Sigma Koki, 30 H). Reaction time was 6 h. Yields based on the initial concentration of the substrate. [b] The reaction was carried out after 30 min of N_2 bubbling. [c] The reaction proceeded after 30 min of O_2 bubbling. [d] DPPA ($7.5 \times 10^{-2} \text{ M}$) was used as the azide source. [e] NaN_3 ($7.5 \times 10^{-2} \text{ M}$) in mixed solvent ($\text{CH}_3\text{CN}:\text{H}_2\text{O} = 4:1$) was used. [f] $\text{TiO}_2 = 5.0 \text{ mg}$ was used as the catalyst in place of the $\text{Rh}^{3+}/\text{TiO}_2$. [g] Light source: black light, $\lambda_{\text{max}} = 365 \text{ nm}$, 1.5 mWcm^{-2} . [h] $[\text{DMPO}] = 1.0 \times 10^{-1} \text{ M}$. [i] Recycled $\text{Rh}^{3+}/\text{TiO}_2 = 5.0 \text{ mg}$ was used as the catalyst.

2% without the $\text{Rh}^{3+}/\text{TiO}_2$ catalyst. In addition, this reaction cannot proceed without $i\text{-Pr}_2\text{NEt}$ (entry 3 in Table 2) or without visible light irradiation (entry 4 in Table 2). Based on these results, it was found that the $\text{Rh}^{3+}/\text{TiO}_2$, the $i\text{-Pr}_2\text{NEt}$, and visible light irradiation are necessary to promote this reaction. Under N_2 atmosphere (30 min of N_2 bubbling before the reaction), the yield of **2** dramatically decreased to 7% due to the lack of an O_2 source (entry 5 in Table 2). The product **2** was obtained in 18% yield under too high O_2 condition (entry 6 in Table 2). Because O_2 should accept the excited electron from the C.B. of the $\text{Rh}^{3+}/\text{TiO}_2$, the reduction of **1** was prohibited in the presence of excess amount of O_2 [32]. Therefore, we concluded that the reaction in air was the best for the benzoyl azide formation. The azide source also influenced the reaction yield. The TMS-N_3 was a superior reagent for the **2** formation in the present system because the yield of **2** was 48% for the reaction with the DPPA (entry 7 in Table 2). The yield of product **2** also decreased to 7% when NaN_3 was used instead of TMS-N_3 (entry 8 in Table 2). When the bare TiO_2 was used as the photocatalyst instead of $\text{Rh}^{3+}/\text{TiO}_2$, the product yield decreased to 28% (entry 9 in Table 2). The modification of the rhodium ion on the TiO_2 is significant for the visible light-driven synthesis. Only 7% yield of **2** was obtained with UV light irradiation ($\lambda_{\text{max}} = 365 \text{ nm}$) because the product of **2** could be decomposed by the irradiation of UV light (entry 10 in Table 2). This result strongly suggested that the importance of the utilization of visible light for the photocatalytic organic synthesis. The reaction was also suppressed in the presence of 5,5-dimethyl-1-pyrroline *N*-oxide (DMPO) as a radical trapping reagent, which suggested the radical may be formed from the substrate **1** during the reaction (entry 11 in Table 2). To evaluate the recyclability of the $\text{Rh}^{3+}/\text{TiO}_2$, the $\text{Rh}^{3+}/\text{TiO}_2$ was collected after the reaction. The collected $\text{Rh}^{3+}/\text{TiO}_2$ exhibited the visible light absorption (Figure S2) and was applied in the catalytic reaction. As a result, **2** was produced in 61% yield (entry 12 in Table 2), which shows that the $\text{Rh}^{3+}/\text{TiO}_2$ is recyclable photocatalyst.

To investigate the effect of the modified metal ions, $\text{M}^{n+}/\text{TiO}_2$ s, such as $\text{Fe}^{2+}/\text{TiO}_2$, $\text{Mg}^{2+}/\text{TiO}_2$, and $\text{Al}^{3+}/\text{TiO}_2$, were synthesized as visible light-responsive photocatalysts by the same procedure with $\text{Rh}^{3+}/\text{TiO}_2$. The loading amounts of these metal ions (Fe^{2+} , Mg^{2+} , Al^{3+}) were similar to Rh^{3+} ion (Table S5). These $\text{M}^{n+}/\text{TiO}_2$ s were used as photocatalysts for the benzoyl azide (**2**) formation instead of the $\text{Rh}^{3+}/\text{TiO}_2$. Although the

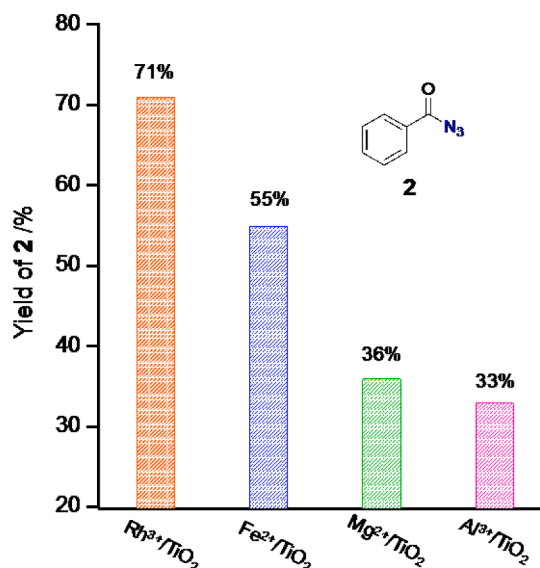


Fig. 4. Difference in photocatalytic activity for the formation of **2**. Conditions: $\text{M}^{n+}/\text{TiO}_2 = 5.0 \text{ mg}$ (Rh^{3+} ion: $2.7 \times 10^{-5} \text{ M}$, Fe^{2+} ion: $3.0 \times 10^{-5} \text{ M}$, Mg^{2+} ion: $3.6 \times 10^{-5} \text{ M}$, Al^{3+} ion: $2.8 \times 10^{-5} \text{ M}$), **1** = $7.5 \times 10^{-3} \text{ M}$, $[\text{TMS-N}_3] = 7.5 \times 10^{-2} \text{ M}$ (10 equiv.), $[i\text{-Pr}_2\text{NEt}] = 5.0 \times 10^{-2} \text{ M}$ (6.5 equiv.), solvent: CH_3CN , light source: 200 W tungsten lamp with 42 L cut-off filter ($\lambda \geq 420 \text{ nm}$) and a heat cut-off filter (Sigma Koki, 30 H). Reaction time was 6 h. Yields based on the initial concentration of the substrate.

benzoyl azide formation was promoted by the other $\text{M}^{n+}/\text{TiO}_2$ s, however, the efficiency of these reactions was lower than the reaction mediated by the $\text{Rh}^{3+}/\text{TiO}_2$ (Fig. 4). The high reactivity of the $\text{Rh}^{3+}/\text{TiO}_2$ for the benzoyl azide formation was estimated by the difference in the reduction potential of the metal ions. Because the rhodium ion has a rather more positive reduction potential than the C.B. of TiO_2 , the rhodium ion site on the $\text{Rh}^{3+}/\text{TiO}_2$ can also work as a reductive site for the substrate [17]. Therefore, the $\text{Rh}^{3+}/\text{TiO}_2$ may show a higher

Table 3

Substrate scope of the benzoyl azides formation.

Entry	Substrate	Product	Time / h	Yield / %
1			6	71
2			3	57
3			2	70
4			10	56
5			1	45
6 ^[b]			3	21
7 ^[b]			3	21

[a] Conditions: $\text{Rh}^{3+}/\text{TiO}_2 = 5.0 \text{ mg}$ (Rh^{3+} ions: $2.7 \times 10^{-5} \text{ M}$), $[\text{Substrate}] = 7.5 \times 10^{-3} \text{ M}$, $[\text{TMS-N}_3] = 7.5 \times 10^{-2} \text{ M}$ (10 equiv.), $[\text{i-Pr}_2\text{NEt}] = 5.0 \times 10^{-2} \text{ M}$ (6.5 equiv.), solvent: CH_3CN , light source: 200 W tungsten lamp with 42 L cut-off filter ($\lambda \geq 420 \text{ nm}$) and a heat cut-off filter (Sigma Koki, 30 H). Yields was determined based on the initial concentration of the substrate. [b] $[\text{Substrate}] = 3.0 \times 10^{-3} \text{ M}$.

reactivity to the substrate than the other $\text{M}^{n+}/\text{TiO}_2$ s for the benzoyl azide formation.

3.3. Substrate scope of the benzoyl azides formation

Benzotrichloride derivatives, which have substituents on the benzene ring, were used for the benzoyl azides formation mediated by the $\text{Rh}^{3+}/\text{TiO}_2$ under visible light irradiation. When the 4-

chlorobenzotrichloride (**3**) was used as a substrate, the 4-chlorobenzoyl azide (**4**) was produced in 31% yield after 6 h of irradiation. The yield of **4** was lower than the yield of **2** because the product **4** might have been over-reacted by the $\text{Rh}^{3+}/\text{TiO}_2$ during the visible light irradiation. Based on this result, we investigated the optimized reaction time for the substrate **3** and the product **4** was obtained in 57% yield after 3 h of irradiation (entry 2 in Table 3). Several benzotrichloride derivatives (**5**, **7**, **9**) were also converted to the corresponding benzoyl azides (**6**, **8**, **10**) in

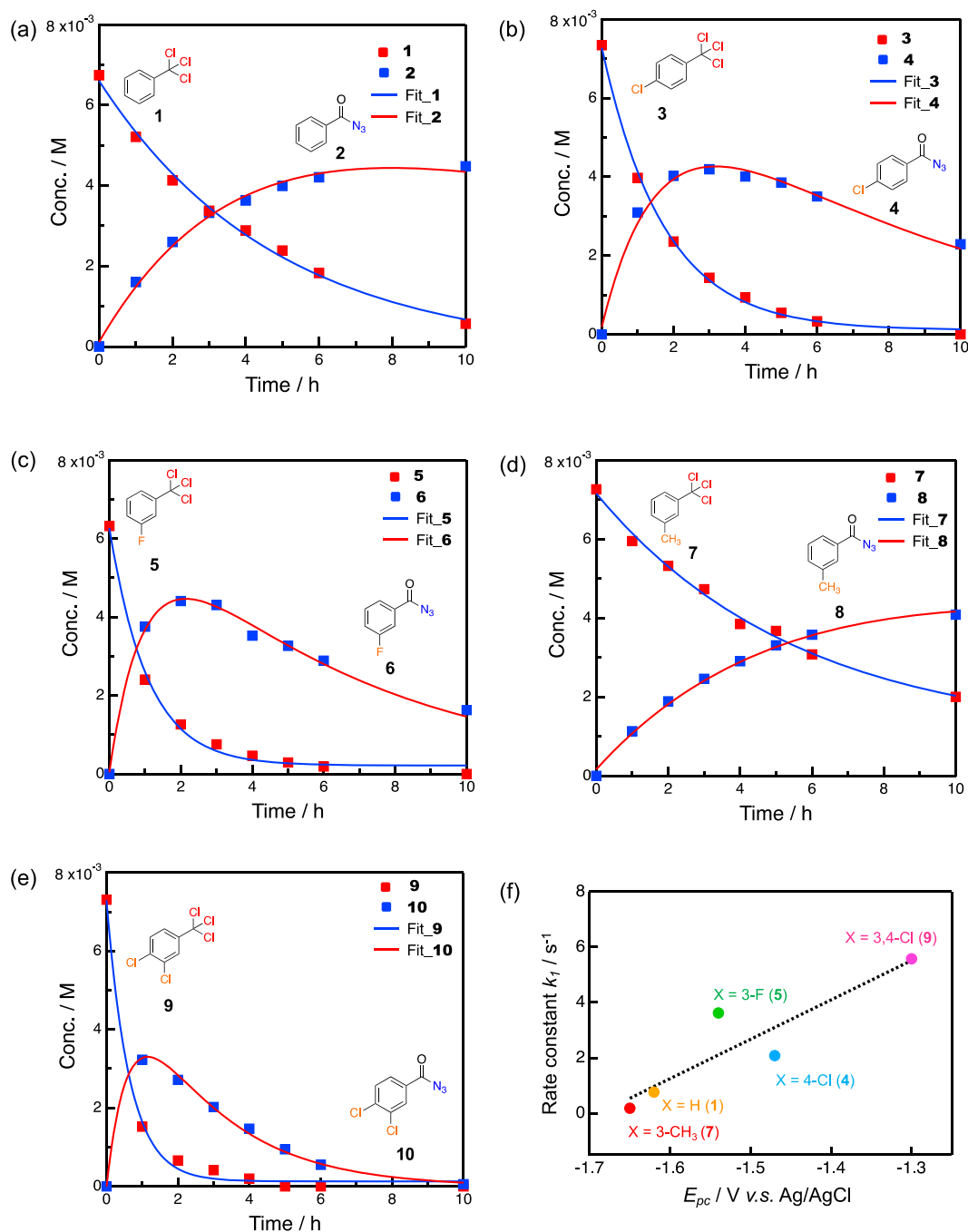


Fig. 5. Reaction profiles of benzoyl azides formation from benzotrichlorides. (a) Benzoyl azide (2), (b) 4-chlorobenzoyl azide (4), (c) 3-fluorobenzoyl azide (6), (d) 3-methylbenzoyl azide (8), and (e) 3,4-dichlorobenzoyl azide (10), (f) plot of E_{pc} vs. k_1 .

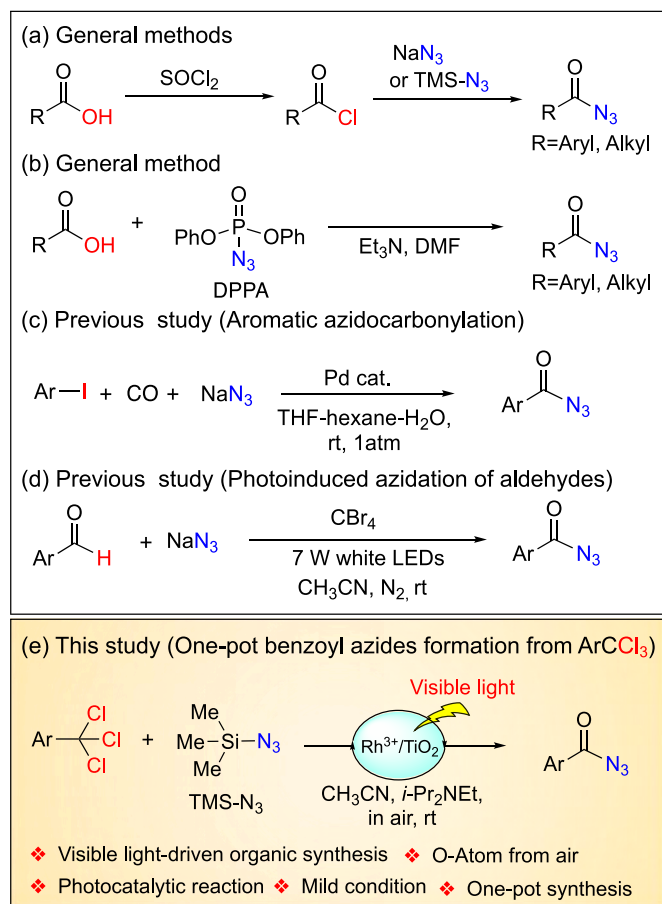
moderate yields at the optimized reaction time (entries 3–5 in Table 3). Moreover, the bis(trichloromethyl)benzene derivatives (11, 13) were also used as substrates for this reaction and the products, which have two acyl azide groups (12, 14), were produced in 21% yield (entries 6–7 in Table 3). These products have a high importance because these compounds can be utilized as building blocks for the synthesis of polymer materials.

A kinetic analysis was carried out on these azides formation catalyzed by the $\text{Rh}^{3+}/\text{TiO}_2$. The time profiles of these reactions were recorded as shown in Figs. 5(a)–(e) and these results were fitted by the curve fitting method of the consecutive reaction to determine the rate constants of k_1 and k_2 (Table 4). Interestingly, the rate constants were quite different between these substrates and there is a good correlation

between the k_1 and the redox potential (E_{pc}) of the substrates (Fig. 5(f)). This result strongly suggested that the rate determining step could be the reduction of the substrates by the SET from the $\text{Rh}^{3+}/\text{TiO}_2$.

3.4. Mechanistic study of the benzoyl azide formation

We investigated the reaction mechanism of this reaction. The cyclic voltammetry of the benzotrichloride (1) and the TMS- N_3 was measured and the redox potentials of 1 and TMS- N_3 were $E_{pc} = -1.6$ V and $E_{pc} = -2.2$ V vs. Ag/AgCl, respectively (Figure S3 and S4). These results can explain that only the substrate can be effectively reduced by the $\text{Rh}^{3+}/\text{TiO}_2$ during visible light irradiation because the energy level of the C.B. ($E_{C.B.}$) is -2.0 V vs. Ag/AgCl in CH_3CN [33]. The reaction with DMPO as a



Scheme 1. Overview of acyl azides formation.

radical trapping reagent cannot efficiently proceed (entry 11 in Table 2), which suggested that the radical species were formed as an intermediate. In addition, the reaction was inhibited in N₂ atmosphere (entry 5 in Table 2). According to this result, the oxygen on the acyl azide group could be derived from the molecular dioxygen (O₂) in air. Based on these results and the literature [28,34], a proposed mechanism was considered as shown in Scheme 4. When the Rh³⁺/TiO₂ was photo-excited by the visible light to produce the excited electrons and the holes based on the charge transfer transient from the rhodium ion to the C.B. on the

TiO₂, and the generated holes accepted electrons from a sacrificial reduction reagent (*i*-Pr₂NEt). The SET occurred from Rh³⁺/TiO₂ to benzotrichloride (1) to provide the dichloromethylphenyl radical II via the radical anion intermediate I. The radical II rapidly reacts with O₂ in air to form the peroxy radical III, and benzoyl chloride VI could be formed via a sequential radical reaction involving intermediates IV and V as described in our previous report. Finally, the reactive intermediate VI should react with TMS-N₃ to form benzoyl azide 2 as the final product. Moreover, the SET step could be regarded as the rate determining step in this reaction based on the kinetic analysis.

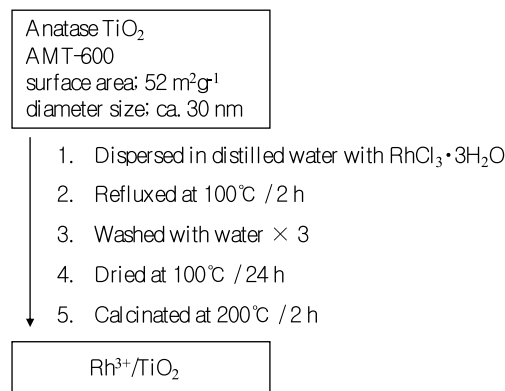
Scheme 3. Preparation of Rh³⁺/TiO₂ particles.

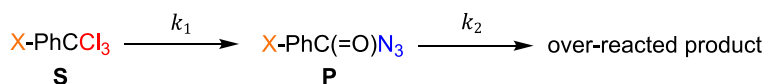
Table 4

Summary of the rate constants and reduction potential of the substrates.^[a]

Substrate (X)	k ₁ / s ⁻¹	k ₂ / s ⁻¹	E _{pc} / V vs. Ag/AgCl ^[b]
1 (H)	0.763	0.267	-1.62
3 (4-Cl)	2.08	0.527	-1.47
5 (3-F)	3.62	0.612	-1.54
7 (3-CH ₃)	0.179	0.0253	-1.65
9 (3,4-Cl)	5.58	1.52	-1.30

[a] Conditions: [substrate] = 1.0 mM, [*n*-Bu₄NPF₆] = 0.1 M, scan rate: 0.1 V/s, solvent: CH₃CN, working electrode: glassy carbon, counter electrode: Pt, reference electrode: Ag/AgCl (3 M NaCl) in N₂.

[b] The E_{1/2} value of ferrocene/ferrocenium (Fc/Fc⁺) was +0.44 V vs. Ag/AgCl with this setup.

The reaction rates of **S**:

$$\frac{d[\text{S}]}{dt} = -k_1 [\text{S}] \quad \dots\dots\dots (1)$$

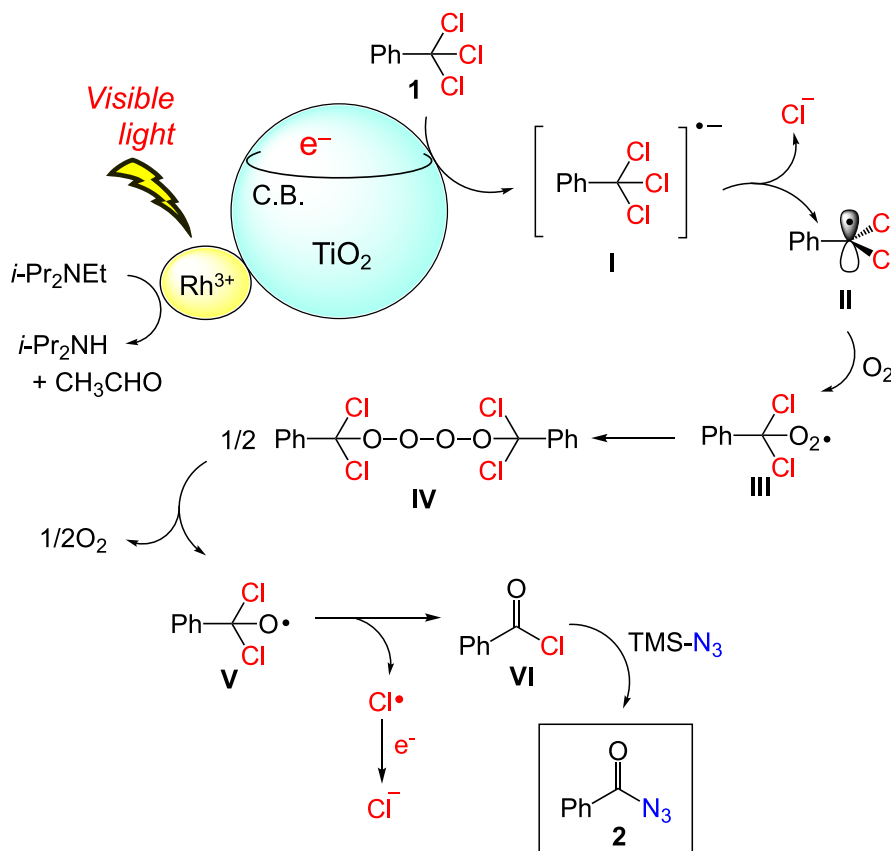
$$[\text{S}] = [\text{S}]_0 \exp(-k_1 t) \quad \dots\dots\dots (2)$$

The reaction rates of **P**:

$$\frac{d[\text{P}]}{dt} = k_1 [\text{S}] - k_2 [\text{P}] \quad \dots\dots\dots (3)$$

$$[\text{P}] = \frac{k_1 [\text{S}]_0}{k_2 - k_1} (\exp(-k_1 t) - \exp(-k_2 t)) \quad \dots\dots (4)$$

Scheme 2. Sequential reaction rate equation for substrate (Eq. 2) and product (Eq. 4).



Scheme 4. Proposed mechanism of benzoyl azide formation from benzotrichloride catalyzed by $\text{Rh}^{3+}/\text{TiO}_2$ under visible light irradiation.

4. Conclusion

In conclusion, we developed visible light-driven benzoyl azides formation catalyzed by $\text{Rh}^{3+}/\text{TiO}_2$ as a new visible light-driven photo-reductive organic synthesis. This one-pot reaction can proceed to form the benzoyl azides in moderate yields under mild conditions at room temperature and at ambient pressure in air. These reactions were recognized with a green and sustainable molecular transformation mediated by the metal ions modified TiO_2 photocatalyst. Furthermore, the photocatalytic N-containing compound formations via the Curtius rearrangement of the benzoyl azide are ongoing in our laboratory.

Appendix A. Supplementary data

Supplementary data to this article can be found online at <https://doi.org/#####/>

Declaration of Competing Interest

The authors declare that they have no known competing financial interests or personal relationships that could have appeared to influence the work reported in this paper.

Data availability

No data was used for the research described in the article.

Acknowledgements

We express our gratitude to Professor Tsuyohiko Fujigaya and Dr. Naoki Tanaka (Kyushu University, Japan) for helping to measure the

XPS, Nissan Chemical Corporation for the TEM images, and Otsuka Electronics Co., Ltd., for the zeta potential. This study was partially supported by JSPS KAKENHI Grant Numbers JP19H02735 (Grant-in-Aid for Scientific Research (B) for H. S.), and JP 21J21004 (for K. S.). Part of the study was performed under the Cooperative Research Program of “Network Joint Research Center for Materials and Devices: Dynamic Alliance for Open Innovation Bridging Human, Environment and Materials” (20224017) and a Grant from the Takahashi Industrial and Economic Research Foundation (12–003–310).

Supplementary materials

Supplementary material associated with this article can be found, in the online version, at doi:[10.1016/j.jpap.2023.100170](https://doi.org/10.1016/j.jpap.2023.100170).

References

- [1] A. Fujishima, K. Honda, Electrochemical photolysis of water at a semiconductor electrode, *Nature* 238 (1972) 37–38, <https://doi.org/10.1038/238038a0>.
- [2] W. Rong, H. Kazuhito, F. Akira, C. Makoto, K. Eiichi, K. Astushi, S. Mitsuhide, W. Toshiya, Light-induced amphiphilic surfaces, *Nature* 338 (1997) 431–432, <https://doi.org/10.1038/41233>.
- [3] A. Fujishima, T.N. Rao, D.A. Tryk, Titanium dioxide photocatalysis, *J. Photochem. Photobiol. C Photochem. Rev.* 1 (2000) 1–21, [https://doi.org/10.1016/S1389-5567\(00\)00002-2](https://doi.org/10.1016/S1389-5567(00)00002-2).
- [4] J. Schneider, M. Matsuoka, M. Takeuchi, J. Zhang, Y. Horiuchi, M. Anpo, D. W. Bahnemann, Understanding TiO_2 photocatalysis: mechanisms and materials, *Chem. Rev.* 114 (2014) 9919–9986, <https://doi.org/10.1021/cr5001892>.
- [5] A. Ajmal, I. Majeed, R.N. Malik, H. Idriss, M.A. Nadeem, Principles and mechanisms of photocatalytic dye degradation on TiO_2 based photocatalysts: a comparative overview, *RSC Adv.* 4 (2014) 37003–37026, <https://doi.org/10.1039/c4ra06658h>.
- [6] M. Ni, M.K.H. Leung, D.Y.C. Leung, K. Sumathy, A review and recent developments in photocatalytic water-splitting using TiO_2 for hydrogen production, *Renew. Sustain. Energy Rev.* 11 (2007) 401–425, <https://doi.org/10.1016/j.rser.2005.01.009>.

- [7] S.P. Pitre, T.P. Yoon, J.C. Scaiano, Titanium dioxide visible light photocatalysis: surface association enables photocatalysis with visible light irradiation, *Chem. Commun.* 53 (2017) 4335–4338, <https://doi.org/10.1039/c7cc01952a>.
- [8] Q. Zhu, D.G. Nocera, Photocatalytic hydromethylation and hydroalkylation of olefins enabled by titanium dioxide mediated decarboxylation, *J. Am. Chem. Soc.* 142 (2020) 17913–17918, <https://doi.org/10.1021/jacs.0c08688>.
- [9] S. Sato, Photocatalytic activity of NO_x-doped TiO₂ in the visible light region, *Chem. Phys. Lett.* 123 (1986) 126–128, [https://doi.org/10.1016/0009-2614\(86\)87026-9](https://doi.org/10.1016/0009-2614(86)87026-9).
- [10] R. Asahi, T. Morikawa, T. Ohwaki, K. Aoki, Y. Taga, Visible-light photocatalysis in nitrogen-doped titanium oxides, *Science* 293 (2001) 269–271, <https://doi.org/10.1126/science.1061051>.
- [11] H. Park, Y. Park, W. Kim, W. Choi, Surface modification of TiO₂ photocatalyst for environmental applications, *J. Photochem. Photobiol. C Photochem. Rev.* 15 (2013) 1–20, <https://doi.org/10.1016/j.jphotochemrev.2012.10.001>.
- [12] H. Kisch, L. Zang, C. Lange, W.F. Maier, C. Antonius, D. Meissner, Modified, amorphous titania - a hybrid semiconductor for detoxification and current generation by visible light, *Angew. Chem. Int. Ed.* 37 (1998) 3034–3036, [https://doi.org/10.1002/\(SICI\)1521-3773\(19981116\)37:21<3034::AID-ANIE3034>3.0.CO;2-2](https://doi.org/10.1002/(SICI)1521-3773(19981116)37:21<3034::AID-ANIE3034>3.0.CO;2-2).
- [13] R. Nakamura, A. Okamoto, H. Osawa, H. Irie, K. Hashimoto, Design of all-inorganic molecular-based photocatalysts sensitive to visible light: Ti(IV)-O-Ce(III) bimetallic assemblies on mesoporous silica, *J. Am. Chem. Soc.* 129 (2007) 9596–9597, <https://doi.org/10.1021/ja073668n>.
- [14] H. Irie, S. Miura, R. Nakamura, K. Hashimoto, A novel visible-light-sensitive efficient photocatalyst, Cr III-grafted TiO₂, *Chem. Lett.* 37 (2008) 252–253, <https://doi.org/10.1246/cl.2008.252>.
- [15] K. Hashimoto, K. Sumida, S. Kitano, K. Yamamoto, N. Kondo, Y. Kera, H. Kominami, Photo-oxidation of nitrogen oxide over titanium(IV) oxide modified with platinum or rhodium chlorides under irradiation of visible light or UV light, *Catal. Today* 144 (2009) 37–41, <https://doi.org/10.1016/j.cattod.2008.12.025>.
- [16] S. Kitano, K. Hashimoto, H. Kominami, Photocatalytic degradation of 2-propanol under irradiation of visible light by nanocrystalline titanium(IV) oxide modified with rhodium ion using adsorption method, *Chem. Lett.* 39 (2010) 627–629, <https://doi.org/10.1246/cl.2010.627>.
- [17] F. Kuttassery, D. Yamamoto, S. Mathew, S.N. Remello, A. Thomas, Y. Nabetani, A. Iwase, A. Kudo, H. Tachibana, H. Inoue, Photochemical hydrogen evolution on metal ion surface-grafted TiO₂-particles prepared by sol/gel method without calcination, *J. Photochem. Photobiol. A Chem.* 358 (2018) 386–394, <https://doi.org/10.1016/j.jphotochem.2017.09.048>.
- [18] S. Bräse, C. Gil, K. Knepper, V. Zimmermann, Organic azides: an exploding diversity of a unique class of compounds, *Angew. Chem. Int. Ed.* 44 (2005) 5188–5240, <https://doi.org/10.1002/anie.200400657>.
- [19] A.K. Ghosh, A. Sarkar, M. Brindisi, The Curtius rearrangement: mechanistic insight and recent applications in natural product syntheses, *Org. Biomol. Chem.* 16 (2018) 2006–2027, <https://doi.org/10.1039/c8ob00138c>.
- [20] A.K. Ghosh, M. Brindisi, A. Sarkar, The Curtius rearrangement: applications in modern drug discovery and medicinal chemistry, *ChemMedChem* 13 (2018) 2351–2373, <https://doi.org/10.1002/cmdc.201800518>.
- [21] D.E. Horning, J.M. Muchowski, The dimethyl formamide – acyl halide complex and its application to the synthesis of acyl azides, *Can. J. Chem.* 45 (1967) 1247–1251, <https://doi.org/10.1139/v67-204>.
- [22] J.H. Macmillan, S.S. Washburne, Interaction of carbonyl compounds with organometallic azides. V. Sorboyl chloride and its conversion to an α -pyridone, *J. Org. Chem.* 38 (1973) 2982–2984, <https://doi.org/10.1021/jo00957a013>.
- [23] T. Shioiri, K. Ninomiya, S. Yamada, Diphenylphosphoryl Azide, A new convenient reagent for a modified Curtius reaction and for the peptide synthesis, *J. Am. Chem. Soc.* 94 (1972) 6203–6205, <https://doi.org/10.1021/ja00772a052>.
- [24] F.M. Miloserdov, V.V. Grushin, Palladium-catalyzed aromatic azidocarbonylation, *Angew. Chem. Int. Ed.* 51 (2012) 3668–3672, <https://doi.org/10.1002/anie.201200078>.
- [25] F.M. Miloserdov, C.L. McMullin, M.M. Belmonte, J. Benet-Buchholz, V. I. Bakmutov, S.A. Macgregor, V.V. Grushin, The challenge of palladium-catalyzed aromatic azidocarbonylation: from mechanistic and catalyst deactivation studies to a highly efficient process, *Organometallics* 33 (2014) 736–752, <https://doi.org/10.1021/om401126m>.
- [26] V.K. Yadav, V.P. Srivastava, L.D.S. Yadav, Visible light induced azidation of aldehydic C-H with carbon tetrabromide and sodium azide, *Tetrahedron Lett* 57 (2016) 2502–2505, <https://doi.org/10.1016/j.tetlet.2016.04.098>.
- [27] K. Shichijo, M. Fujitsuka, Y. Hisaeda, H. Shimakoshi, Visible light-driven photocatalytic duet reaction catalyzed by the B₁₂-rhodium-titanium oxide hybrid catalyst, *J. Organomet. Chem.* 907 (2020) 121058–121062, <https://doi.org/10.1016/j.jorganchem.2019.121058>.
- [28] K. Shichijo, M. Watanabe, Y. Hisaeda, H. Shimakoshi, Development of visible light-driven hybrid catalysts composed of earth abundant metal ions modified TiO₂ and B₁₂ complex, *Bull. Chem. Soc. Jpn.* 95 (2022) 1016–1024, <https://doi.org/10.1246/bcsj.20220080>.
- [29] K. Saito, T. Umi, T. Yamada, T. Suga, T. Akiyama, Niobium(v)-catalyzed defluorinative triallylation of α,α,α -trifluorotoluene derivatives by triple C-F bond activation, *Org. Biomol. Chem.* 15 (2017) 1767–1770, <https://doi.org/10.1039/c6ob02825j>.
- [30] C. Jen-Yuan, Kinetic analysis of irreversible consecutive reactions, *J. Am. Chem. Soc.* 70 (1948) 2256–2261, <https://doi.org/10.1021/ja01186a078>.
- [31] K. Tamai, S. Hosokawa, H. Asakura, K. Teramura, T. Tanaka, Low-temperature NO_x trapping on alkali or alkaline earth metal modified TiO₂ photocatalyst, *Catal. Today* 332 (2019) 76–82, <https://doi.org/10.1016/j.cattod.2018.07.045>.
- [32] C.C. Nguyen, C.T. Dinh, T.O. Do, Hollow Sr/Rh-codoped TiO₂ photocatalyst for efficient sunlight-driven organic compound degradation, *RSC Adv.* 7 (2017) 3480–3487, <https://doi.org/10.1039/c6ra25987a>.
- [33] M. Cherevatskaya, M. Neumann, S. Földner, C. Harlander, S. Kümmel, S. Dankesreiter, A. Pfützner, K. Zeitler, B. König, Visible-light-promoted stereoselective alkylation by combining heterogeneous photocatalysis with organocatalysis, *Angew. Chem. Int. Ed.* 51 (2012) 4062–4066, <https://doi.org/10.1002/anie.201108721>.
- [34] Z. Luo, K. Imamura, Y. Shiota, K. Yoshizawa, Y. Hisaeda, H. Shimakoshi, One-pot synthesis of tertiary amides from organic trichlorides through oxygen atom incorporation from air by convergent paired electrolysis, *J. Org. Chem.* 86 (2021) 5983–5990, <https://doi.org/10.1021/acs.joc.1c00161>.